Reduction in dislocation density and strain in GaN thin films grown via maskless pendeo-epitaxy

A.M. ROSKOWSKI[1], E.A. PREBLE[2], S. EINFELDT[2,3], P.M. MIRAGLIA[2], J. SCHUCK[4], R. GROBER[4], and R.F. DAVIS[*2]

[1]Department of Chemical Engineering, Box 7919, North Carolina State University, Raleigh, NC 27695, USA
[2]Department of Materials Science and Engineering, Box 7907, North Carolina State University, Raleigh, NC 27695, USA
[3]Institute of Solid State Physics, P.O. Box 330440, University of Bremen, 28334 Bremen, Germany
[4]Department of Applied Physics, Yale University, New Haven, CT 06520, USA

Maskless pendeo-epitaxy (PE) involves the lateral and, commonly, the vertical growth of cantilevered "wings" of material from the side-walls of unmasked etched forms. Cross-sectional SEM micrographs revealed that films grown at 1020°C exhibited similar vertical [0001] and lateral [11$\bar{2}$0] growth rates. Increasing the temperature increased the latter due to the higher thermal stability of the GaN(11$\bar{2}$0). The (11$\bar{2}$0) surface was atomically smooth under all growth conditions with an RMS = 0.17 nm. High resolution X-ray diffraction (HRXRD) and atomic force microscopy of the PE films confirmed transmission electron microscopy results regarding the reduction in dislocation density in the wings. Measurement of strain indicated that the wing material is crystallographically relaxed as evidenced by the increase in the c-axis lattice parameter and the upward shift of the E2 Raman line frequency. However, tilting of the wings of ≤ 0.15° occurred due to the tensile stresses in the stripes induced by the mismatch in the coefficients of thermal expansion between the GaN and the underlying substrate.

Keywords: pendeo-epitaxy, gallium nitride, metalorganic vapour phase epitaxy, lateral growth rate, vertical growth rate, dislocations, strain, relaxation, wing tilting, atomic force microscopy, X-ray diffraction, photoluminescence, Raman.

1. Introduction

Dislocations in GaN and related nitride films primarily accommodate residual stresses generated by the misfits in lattice parameters and coefficients of thermal expansion between the nitride materials and the substrates on which they are heteroepitaxially grown. These defects occur in densities of ~10^9 cm^{-2} and (1) produce energy levels in the band gap that combine with charge carriers (electrons) from donor states and states at the bottom of the conduction band, (2) act as conduits for charge transport that result in high leakage currents and slow breakdown of rectifying contacts and (3) reduce significantly the lifetime of laser diodes. Several research groups have determined that lateral epitaxial overgrowth (LEO) and pendeo-epitaxy (PE) can significantly reduce the dislocation density in GaN and AlGaN films grown on sapphire [1–5] and SiC [6–14] Pendeo-epitaxy is an overgrowth technique in which the stripes and/or other "seed" forms are etched through the nitride material and into the substrate. GaN or AlGaN is again grown either laterally and then vertically over a mask [Fig. 1(a)] or laterally and vertically from the stripe material [Fig. 1(b)]. The threading dislocation density in the laterally grown sidewall regions is reduced to ~10^5 cm^{-2} relative to the initial GaN stripe.

Initial pendeo-epitaxy research involved the deposition of an amorphous silicon nitride mask on the GaN seed film prior to etching. The GaN regrown on the etched form(s) did not nucleate either on the SiC substrate or on the silicon nitride mask at the higher temperatures employed to enhance lateral growth. Therefore, deposition was forced to selectively begin on the sidewalls [11–15] and the masks confined the threading dislocations originating from the heteroepitaxial growth to their original stripes. This process route enabled growth of continuous films of GaN and AlGaN on SiC [8,11,15] and Si(111) [10] substrates to be realised. However, the growth fronts over the masked regions were tilted. As a consequence, vertical boundaries formed above each mask during the coalescence of these growth fronts, due to the misregistry of the material. The presence of two crystallographic orientations tilted towards
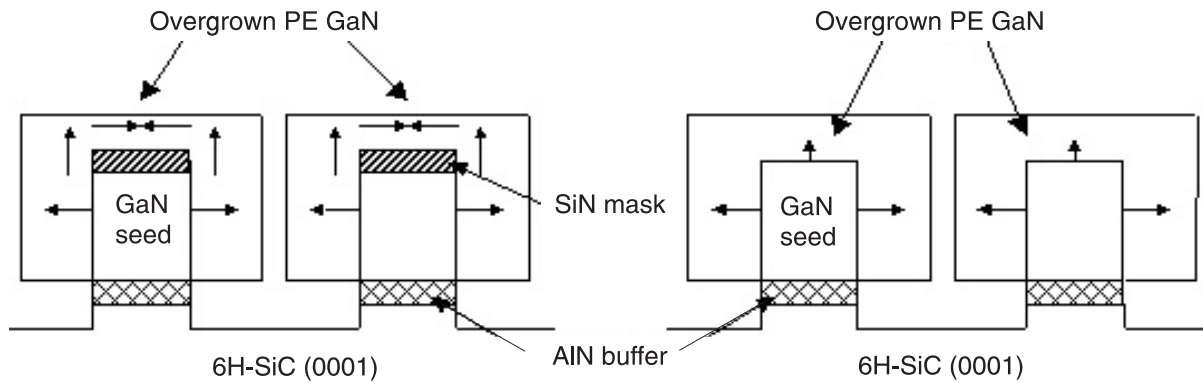
*e-mail: robert_davis@ncsu.edu

Fig. 1. Schematic of: (a) PE growth from GaN seed laterally off the sidewalls then vertically and laterally over the silicon nitride mask; (b) PE growth from GaN seed laterally off the sidewalls and vertically off the stripe.

each other has also been reported in GaN films grown via LEO [4,16–18].

Recent research efforts have centred on PE growth without the use of a silicon nitride mask, termed "maskless" PE. Lateral and vertical growth is initiated from the GaN stripe, as depicted in Fig. 1(b). The elimination of a growth mask has several advantages: the crystallographic tilt described above that occurs in the overgrown material is significantly reduced, a source for impurities in the overgrowth material is eliminated and PE growth of AlGaN films can be realised. Although AlGaN nucleates on the SiC substrate, sufficiently deep trenches are made to prevent contact between the material growing vertically from the bottom of the trench and the material growing laterally from the sidewalls of the stripes [10].

In essence, PE is a new approach to selective epitaxy of GaN and AlGaN layers that incorporates mechanisms of growth exploited by the conventional LEO process, but usually alleviates the mask alignment problems through the use of the substrate itself as a pseudo-mask. The following Sections describe the recent advancements concerning the effect of growth parameters on growth rates, surface microstructure, the reduction in defects and strain, and the structural and optical characteristics of maskless GaN thin films grown via PE.

2. Experimental

Each AlN buffer layer, GaN seed layer and maskless PE GaN and/or AlGaN layer was sequentially grown on a 6H-SiC(0001) substrate in a cold-walled, vertical, pan-

Fig. 2. Composite of cross-sectional TEM micrographs of a PE $Al_{0.1}Ga_{0.9}N$ film. Note the threading dislocations continue from the GaN stripes into the film.

cake-style metalorganic vapour phase epitaxy (MOVPE) system. The 100-nm thick AlN buffer layers and the 1-µm thick GaN seed layers were grown at 20 Torr and platter temperatures of 1120°C and 1020°C, respectively. The precursor species (mass flow rates) of tri-methylaluminum (TMA; 5.4 µmol/min), tri-ethylgallium (TEG; 101 µmol/min) and ammonia (NH$_3$; 0.14 mol/min) were mixed with a high-purity H$_2$ diluent (3 slm) in a two-inch internal diameter sleeve located two inches above the substrate.

A Ni layer was deposited on patterned photoresist stripes on each GaN seed layer by e-beam evaporation. Etch mask stripes were subsequently produced using standard photolithography lift-off techniques. An inductively coupled plasma (ICP) system and a mixture of Cl$_2$ and BCl$_3$ gases were used to etch the unmasked striped regions through the GaN and the AlN and into the near-surface areas of the SiC substrate. The Ni was then removed using a 5-min dip in HNO$_3$. The remaining GaN seed layer consisted of 2 and 3 µm wide stripes separated by distances of 12 and 7 µm, respectively, and oriented along [11$\bar{2}$0]. The exposed (11$\bar{2}$0) sidewalls and the top (0001) face of the stripes were subsequently dipped in 50% hot HCl to clean the surface prior to regrowth of the PE layer.

The lateral and vertical growth rates of the PE GaN films are very sensitive to temperature and the NH$_3$/TEG (V/III) molar flow rate ratios. As such, the growth of these films was investigated over the ranges of temperature and TEG flow rates of 1040°C–1100°C and 17–100 µmole/min, respectively. The flow rates of the NH$_3$ and the H$_2$ diluent were maintained at 0.14 mol/min and 3 slm, respectively. The total gas flow into the reactor remained constant for all the experiments to assure a uniform laminar flow over the substrate.

Cross-sectional images of the surface microstructure of the wing and stripe material were obtained using scanning electron microscopy (SEM) and were used to calculate the lateral and/or vertical growth rates of these features. Atomic force microscopy (AFM) was employed in the tapping mode to obtain higher resolution micrographs of the growth surface as well as the aerial distribution of dislocations that terminated at the (0001) surface. Defect characterisation and measurements of the strain via changes in lattice parameter were conducted using the results from on- and off-axis rocking curves and reciprocal space mapping acquired via high-resolution x-ray diffraction (HRXRD). Optical characterisation of spatially resolved (≈400 nm) band-edge emission was performed via micro-photoluminescence (PL) at 10 K using a He-Cd (λ = 325 nm) laser. Shifts in the frequency of the E2 line measured at 10 K using an Ar-ion (λ = 488 nm) laser coupled to micro-Raman unit with a spatial resolution of ≈700 nm, revealed discrete regions of strain in the PE films. Micro-Raman spectra of the LO phonon also yielded information regarding the carrier concentration of the overgrown material. Secondary-ion mass spectroscopy (SIMS) depth profiles were obtained to determine the presence and concentrations of carbon, oxygen and silicon in the GaN films.

3. Results and discussion

3.1. Pendeo-epitaxial growth and decomposition on GaN(0001) and (11$\bar{2}$0) surfaces

High lateral growth rates are desired in both LEO and PE techniques to achieve rapid coalescence and commercially viability. Reported factors that increase the lateral growth rate of GaN films in the [11$\bar{2}$0] direction from [1$\bar{1}$00] oriented stripes include growth temperature [12,19], V/III molar flow rate ratio [1,2] and modulation of the NH$_3$ flow rate [5,9].

Figures 3 and 4 are related by the lower case letters in each and show analytically and pictorially, respectively, the effect of growth temperature for two V/III flow rate ratios on the lateral/vertical GaN growth rate ratios (R). The V/III ratio was increased from 1323 to 6160 at all temperatures via reduction in the TEG flow rate from 101.2 µmol/min to 16.7 µmol/min. The most dramatic increase in R occurred for the V/III ratio of 6160 after the growth temperature was increased beyond 1060°C, as shown, e.g., in Fig. 3(d) and the associated Fig. 4(d). However, the roughness of the (0001) surface also increased above an R = 10; as seen in the SEM image, Fig. 4(d), of a sample having a value of R of approximately 24. Additional understanding regarding the changes in the values of R can be obtained by uncoupling the lateral and vertical growth rates and plotting them as a function of temperature in the manner shown in Fig. 5. Calculation of the growth rates from the SEM cross-sectional micrographs shown in Fig. 4 and additional micrographs acquired for the PE GaN films grown at the intermediate temperatures revealed that the lateral growth rate increased with increasing temperature and the vertical growth rate either remained constant or decreased for both V/III ratios. In Fig. 5, the growth rates, both laterally and vertically, are greater for the V/III ratios of 1323 than for the ratio of 6160 due to the larger amount of TEG used in
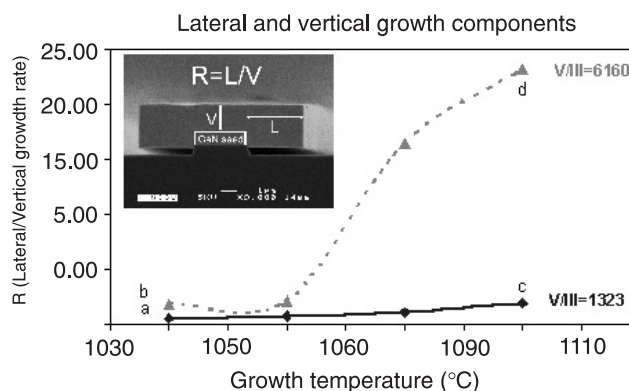

Fig. 3. Ratio of lateral (L)-to-vertical (V) growth rates (R) as a function of growth temperature and V(NH$_3$)/III(TEG) ratio. The NH$_3$ flow rate remained constant. Inset shows how a representative value of R was calculated for these films. The growth time was 1 hr for each point.
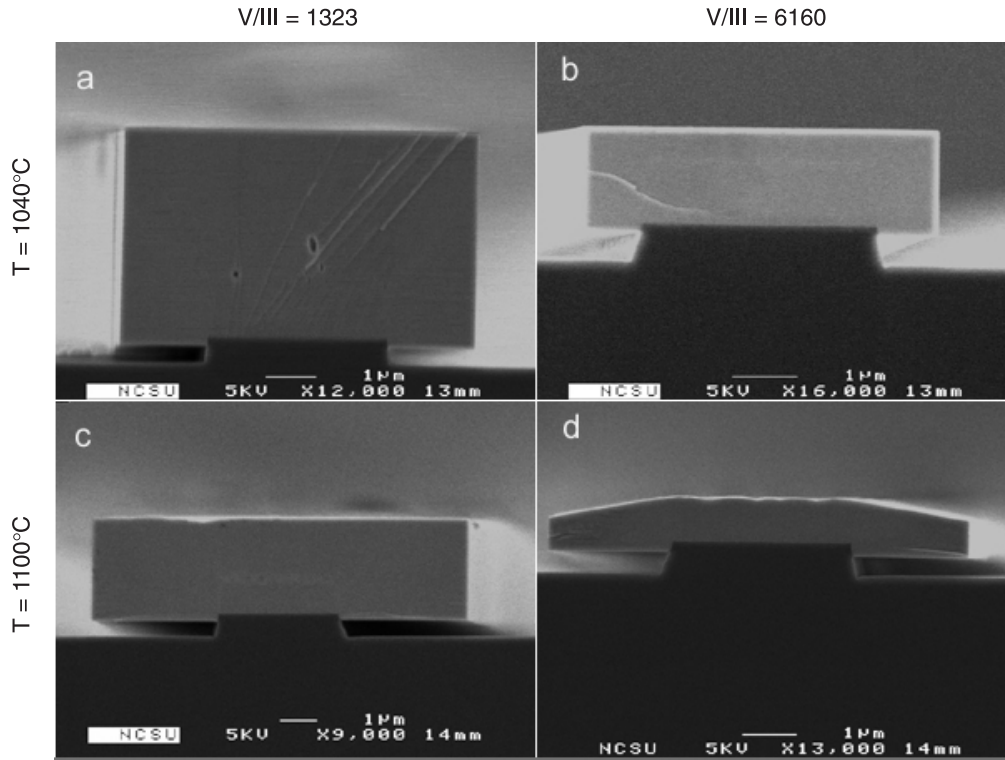
V/III = 1323   V/III = 6160

Fig. 4. Cross-sectional SEM [1$\bar{1}$00] view of uncoalesced PE GaN films grown under different temperatures and V/III gas ratios for 1 hour at 20 torr total pressure. The original GaN seed was 1 μm tall. Note: the magnification for each SEM picture is different.

growth. For V/III ratios of 1323, the vertical growth was dominant over lateral growth at temperatures below ≈1080°C. An increase in lateral growth at 1100°C changed the value of R to greater than 1. The dramatic increase in the value of R above 1 for PE growth at a V/III ratio = 6160 for T > 1060°C occurred due to the drop in the vertical growth rate to near zero. At 1060°C and above, decomposition of the (0001) surface occurred in competition with the vertical growth of GaN; however, it did not affect lateral growth. This competition is obvious in Fig. 4(d) where
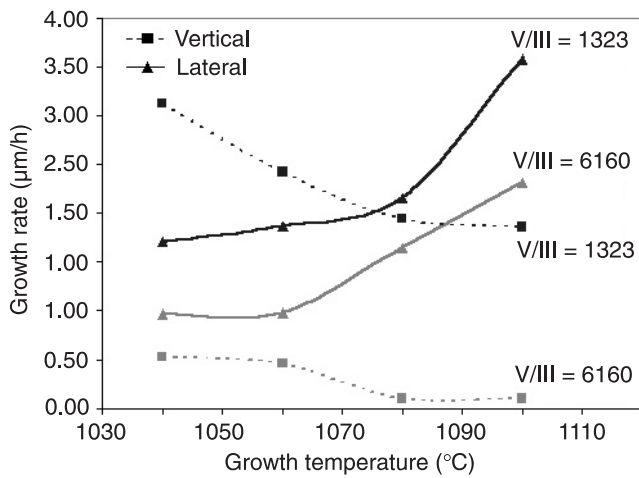

Fig. 5. Lateral and vertical growth rates as a function of growth temperature and V(NH$_3$)/III(TEG) ratio. The NH$_3$ flow rate remained constant.

growth in the [11$\bar{2}$0] has produced large wings off the original seed, but the (0001) surface is rough and very little vertical growth has occurred.

Gallium nitride, despite strong chemical bonding decomposes above 800°C in flowing hydrogen [20], and MOVPE becomes a near equilibrium competitive process between adatom incorporation, desorption into the gas phase and GaN decomposition. This competition was particularly relevant and made complex in the present research, as the PE GaN films were grown at temperatures exceeding those normally employed in the MOVPE of this compound in the presence of both H$_2$ and NH$_3$. This latter gas decomposes to provide atomic nitrogen as well as atomic and additional molecular hydrogen that chemically react with the GaN(0001) surface. An overview of prior research regarding GaN decomposition in H$_2$ and/or NH$_3$ with and without the presence of TEG is given below.

The decomposition of the GaN(0001) surface has been measured by gravimetric means in H$_2$ [21–23] and NH$_3$ [24,25] for pressure ranges of 10–700 torr, which encompasses the range used most commonly in the MOCVD of this material. Rebey *et al.* [21] reported that the decomposition rate at 1050°C increased rapidly with increasing H$_2$ flow rate and at 3 slm reached 30 μm/hr. They measured a critical temperature of 830°C, at which the rate-limiting decomposition process changed from surface kinetics (E$_a$ ~1.87 eV) to diffusion in the boundary layer (E$_a$ ~0.38 eV). They postulated the decomposition sequence for GaN to be (a) the desorption of surface nitrogen
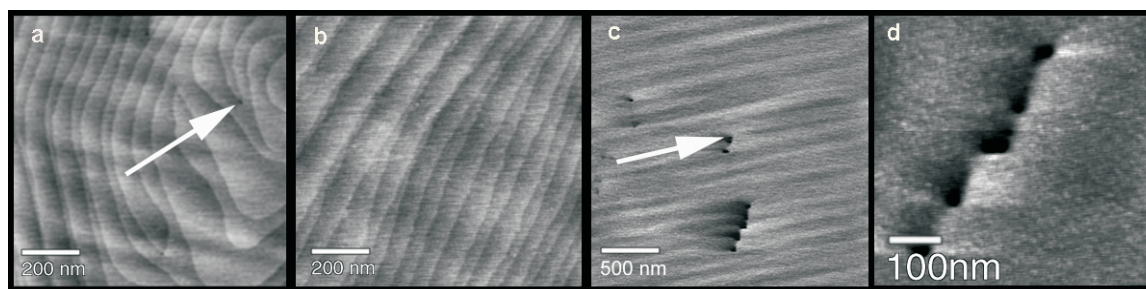
Fig. 6. AFM micrographs acquired from: (a) the (0001) GaN stripe area; (b) the wing GaN (0001) area; (c) the GaN ($11\bar{2}0$) wing face. Arrows in (a) and (c) point to intersections of dislocations at the surface of these respective planes. The striations in (c) are electronic noise from the AFM; step structures have never been observed on this plane.

atoms leading to a Ga-rich surface, (b) the diffusion of bulk nitrogen atoms to the surface, (c) the subsequent formation and desorption of nitrogen molecules, and (d) the formation of Ga droplets.

The results of further studies show that decomposition rates of the GaN(0001) surface at 1000°C in H_2 are reduced two orders of magnitude by the addition of NH_3 as it blocks sites needed for GaN decomposition [23]. For this reason a large NH_3/TEG ratio is used during MOVPE growth. Nitrogen generated from the decomposition of NH_3 must be larger than the desorption flux of N to guarantee a saturation surface coverage of this species [26]. If too much NH_3 is used the number of open surface sites is reduced and the growth rate decreases [27,28]. However, there is a range of NH_3 flow rates wherein the growth rates are controlled by the flux of metal species to the surface of the growing film. This is demonstrated in Fig. 5 by the reduction in vertical growth of the PE samples at all temperatures with a reduction in TEG flow (increase in V/III ratio).

As the growth temperature increases, it is postulated that the role of NH_3 gradually changes from that of a site-blocker to that which provides atomic surface hydrogen via decomposition. This hydrogen reacts with atomic surface nitrogen to form volatile species and consequent decomposition of the GaN. To check this hypothesis that decomposition of GaN(0001) is enhanced under conditions of large NH_3 flow rates, a PE growth run was conducted at 1100°C wherein the TEG flowrate was held constant at 21.7 µmol/min and the NH_3 flow rate increased from 3 slm to 5 slm. Increasing decomposition was manifest in the increasing roughness of the (0001) surface as well as a low vertical growth rate.

Early experiments of GaN growth on different crystallographic orientations of sapphire crystals also showed that ($11\bar{2}0$) has a higher thermal stability than (0001) [29]. This was also borne out in our PE GaN experiments at 1100°C where in growth occurred along [$11\bar{2}0$] and growth and decomposition occurred concomitantly along [0001]. Moreover, no indication of ($11\bar{2}0$) decomposition was observed under any growth conditions at 1100°C including low TEG and high NH_3 flow rates. As such, lateral growth rates along [$11\bar{2}0$] can be controlled solely by temperature.

3.2. Surface microscopy and defects

The GaN(0001) surface is a Ga-terminated polar surface and much is known about growth and decomposition kinetics on this surface, as described above. Growth on an AlN buffer layer initiates with the nucleation of three-dimensional hexagonal islands [30]. Upon coalescence of the islands, GaN growth continues on this surface via a step-flow mechanism, as shown by the results of AFM studies presented in Figs. 6(a) and 6(b). The ($11\bar{2}0$) surface is nonpolar and consists of two surface Ga atoms and two surface N atoms per unit cell [31]. No steps were observed on the ($11\bar{2}0$) plane over a 2.5 µm scan, as shown in Fig. 6(c). A higher resolution image of the ($11\bar{2}0$) surface in Fig. 6(d) also shows the absence of steps. The striations shown in Figs. 6(c) and 6(d) were caused by electronic noise within the AFM. This suggests that either the step height, if steps exist, is less than 0.15 nm or below the noise-limited resolution of the AFM or that the terrace width of the steps is sufficiently small that they cannot be observed by AFM. If steps do not exist, the surface is atomically smooth and lateral growth occurs by some mechanism other than step-flow, possibly via the thermodynamically controlled Frank-van der Merwe (layer-by-layer) mode.

The black dots at the ends of the associated arrows in Figs. 6(a) and 6(c) indicate the termination of dislocations in the (0001) stripe material and the laterally grown ($11\bar{2}0$) surfaces, respectively. The dislocations in the latter surface were only observed near the bottom of the volume of the GaN wings, possibly indicating that they were generated at the vertical interface between the AlN buffer layer and the laterally grown GaN. The dislocation indicated in Fig. 6(a) is also the point of initiation of a heterogeneous step. Heterogeneous steps are steps generated in a terrace on the surface at the point of and due to the intersection of the terrace by a screw and/or mixed-type dislocations [32]. Homogeneous steps are produced by the step-flow growth of the material. Similar dislocations and their associated heterogeneous steps were never observed in the wing regions of the (0001) surface; only homogeneous steps such as those shown in Fig. 6(b) were present.

The presence of dislocations with screw and edge character in the stripe and wing areas were determined via scans of the (0002) and ($11\bar{2}0$) x-ray reflections. The

FWHM values of the rocking curves in the on-axis (0002) reflection indicate the concentration of screw-type dislocations while values of off-axis (30$\bar{3}$2) FWHM determine the relative density of edge-type dislocations [33]. A reduction in screw-type dislocations in the wings with respect to the stripes is indicated by a reduction in FWHM of the (0002) reflections from 646 arcsec to 354 arcsec. The off-axis FWHM of the wing area was 126 arcsec compared to 296 arcsec for the stripe indicating a reduction in the edge-type dislocations as well.

The (0001) surface microstructure was very sensitive to growth temperature, even in regimes of temperature and V/III ratios where (0001) surface decomposition was not prevalent. For our reactor geometry and growth conditions, the optimum temperature for planar growth of conventional GaN films was 1020°C. The rates of coalescence of the growth fronts of the material growing laterally from the sidewalls of the PE stripes were enhanced by an increase in temperature. However, increasing the temperature beyond 1020°C increased the propensity for the growth of spiral hillocks on the (0001) surface within the stepped microstructure [34]. Figures 7(a) and (b) show a comparison of the stepped microstructures obtained on the (0001) surface during PE growth at 1020°C and 1100°C, respectively. The R$_{MS}$ roughness was nearly the same in each case; however, the occurrence of hillocks such as that shown in Fig. 7(b) represents the early stage of growth instability that occurred at elevated temperatures.
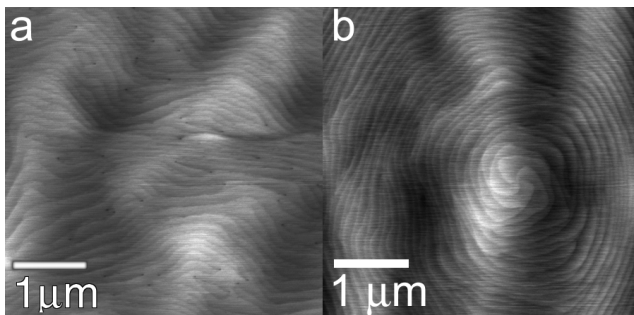

Fig. 7. AFM images obtained from the centre of a stripe region after early stages of coalescence on a pendeo post (3–7 scheme): (a) stable surface formed at 1020°C, R$_{MS}$ = 0.35 nm; (b) unstable surface with quadruple hillock formed during deposition at 1100°C, R$_{MS}$ = 0.31 nm.

Spiral hillocks are a consequence of preferred growth at heterogeneous steps that have their origin at the intersections of the aforementioned dislocations with the (0001) growth surface [35–37]. Stable growth of spiral hillocks occurs under conditions that allow continuous integration of adatoms at steps, if the rate of homogeneous step advancement is synchronous with the rotational velocity of the hillock. For the hillock to be annihilated under steady-state conditions, the advancing homogeneous step must reach the centre of the hillock at the same time that the rotation of the hillock completes one revolution.

Unfortunately, hillocks increase in size due to the large lateral growth rate at high temperatures; they tend to eventually cover the laterally growing areas of the (0001) surface. In many cases of PE growth at T = 1100°C, the vertical growth is solely attributed to hillock growth. As mentioned in the previous section, the desorption flux of N and Ga species increases with an increase in temperature. Therefore, the adatom diffusion length decreases. The probability of adatom condensation at homogeneous steps relative to that at heterogeneous steps decreases with an increase in temperature, and the stable growth of spiral hillocks occurs.

All the hillocks were centred on the stripe regions, i.e., within the areas over the original seed material; no hillocks were observed to originate in the PE overgrowth regions even at the highest growth temperature of 1100°C. An investigation was conducted to observe and characterise the defects above the stripe regions, including the original seed material, as well as in the overgrowth or wing regions. As described above, the AFM studies of the (0001) surface structure of the stripe material revealed heterogeneous steps [see arrow in Fig. 6(a)]. An examination of Fig. 2 reveals no apparent lateral propagation of the vertically oriented threading dislocations from within the stripe region into the wing region. The straight homogeneous steps shown in the AFM micrograph of the (0001) surface in the wing area in Fig. 6(b) indicate the absence of threading dislocations.

A trade-off occurs in PE growth between growth rate and the degradation of the surface microstructure as a result of the growth of the hillocks. Hillock-free PE surfaces can be accomplished at 1020°C at the sacrifice of coalescence time, due to the drop in R at this temperature. For structures that require large overgrowth (>10 μm), the resulting PE GaN films grown at T = 1020°C are very thick upon coalescence and have a greater tendency to crack. However, as the temperature is increased, the surface over the stripes becomes increasingly prone to hillock formation.

Hillocks did not grow on the (11$\bar{2}$0) surface under any conditions, even around the dislocations that intersect this surface, as shown in Figs. 6(c) and 6(d). This indicates that the intersecting dislocations are pure edge in character. The aforementioned thermal stability of this surface may also contribute to the absence of hillocks and in turn the low RMS value.

3.3. Tilt and strain in uncoalesced pendeo-epitaxial GaN

Wing tilt is measured using XRD by measuring an ω rocking curve about the GaN 0002 peak with the scatter plane perpendicular to the stripe. As shown in Fig. 8, reciprocal space maps of the uncoalesced PE material show a centre peak produced by the seed material and two side peaks produced by the two wings when the beam direction is perpendicular to the seed stripe direction. The two wing peaks are
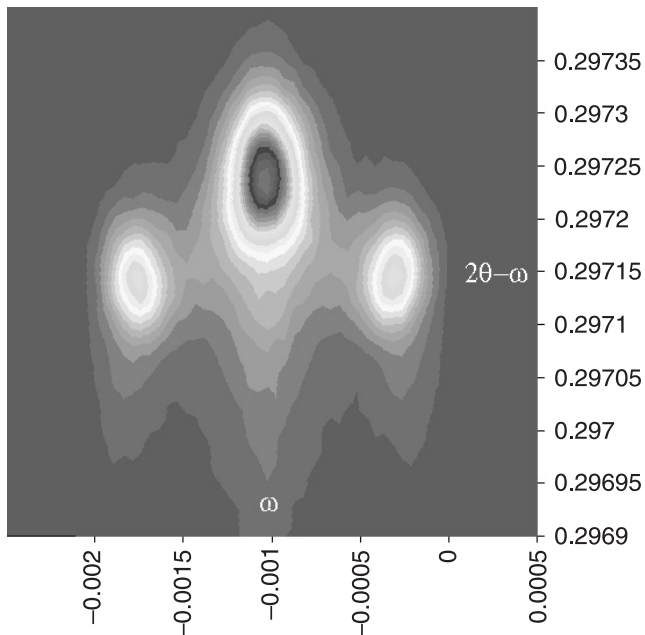
Fig. 8. High resolution XRD reciprocal space map of stripe and wing regions in an uncoalesced pendeo-epitaxial GaN film.

shifted with respect to the seed layer peak in the omega direction as a result of crystal tilt in the wing regions. The 2θ–ω shift is due to strain relaxation in the wing regions.

The origins of the tilt in maskless PE are due to the mismatch in the coefficients of thermal expansion between the GaN stripe material and the SiC substrate. Experimental and theoretical simulations have shown that the crystallographic tilt of GaN is stress-induced [38]. The higher the tensile stress in the stripe region, the higher the wing tilt that is measured by XRD. The strains generated by these stresses cause the wings to bend upward during cooling from the growth temperature. The wing tilt in an uncoalesced PE film heated to 800°C was measured at selected temperatures via high-temperature XRD. The results of this experiment are shown in Fig. 9 [39]. As the temperature increased, the measured wing tilt decreased due to the relax-
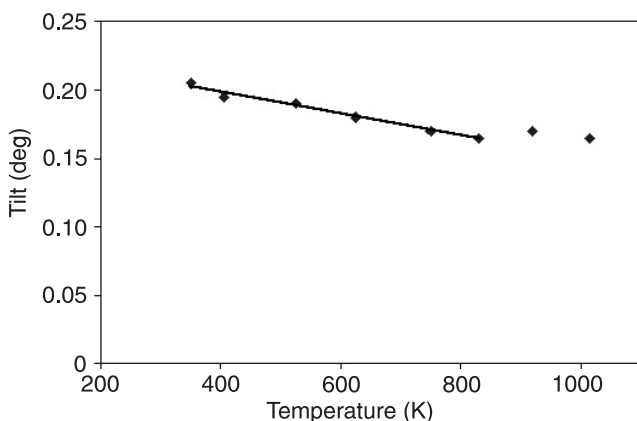

Fig. 9. Plot of crystallographic tilt in uncoalesced PE GaN films, measured by XRD, as a function of film temperature.

ation of the GaN stripe material. The wing tilt is not completely relieved at higher temperatures as seen in Fig. 9. Stress is also induced in the GaN epilayer due to the lattice mismatch between the AlN buffer layer and the GaN thin film. These stresses are not relieved thermally but also contribute to the wing tilt.

Once free of the strain effects caused by the SiC(0001) substrate, a slight relaxation of both the a(–0.07%) and c(+0.03%) lattice parameters was observed in the wing region. In Fig. 8, the two wing peaks are shifted with respect to the seed layer in the ω direction due to strain relaxation in the wing regions. Micro-Raman measurements showed the same strain reduction in the uncoalesced PE wings. An upward shift of the E2 Raman line of approximately 0.7 wavenumbers in the wing area with respect to the stripe was observed in the two-dimension plot of the E2 frequency distribution in Fig. 10 and indicated a relaxation in the former. A change in the c-axis lattice parameter of ~0.02% has been calculated from the frequency shift in the E2 line using the methods developed by Kisielowski and co-workers [40]. The resulting shifts in lattice parameters agree well with the calculated change in the c-axis measured with XRD [41].
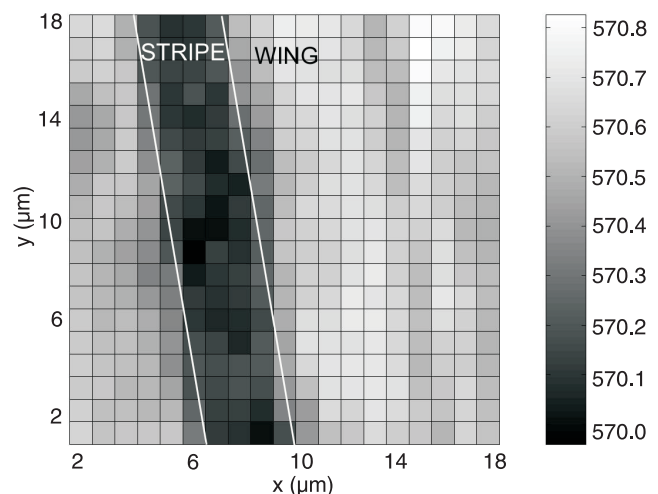

Fig. 10. Two-dimensional plot of Raman line frequency of an uncoalesced PE GaN film (specifically a wing and stripe region). An increase in the line frequency represents a relaxation of strain in the material.

3.4. Optical properties, impurities and carrier concentrations

Another important advantage of PE growth without a mask is the elimination of an impurity source. Analyses of the centre frequency of the coupled LO phonon-plasmon (LPP) in micro-Raman spectra [42] obtained from cross-sections of LEO material showed that regions grown over an SiO_2 mask contain carrier concentrations that exceed 10^{18} cm^{-3}. This is significant evidence of considerable impurity incorporation [43,44]. Micro-Raman spectra of the PE samples grown in the present research showed an uncoupled E1

(LO) phonon at 740 cm^{-1} indicating that the carrier concentration was $<10^{17}$ cm^{-3} in both the wing and the stripe material, as expected for overgrowth without a mask. This was further quantified by secondary ion mass spectrometry (SIMS) ion imaging that showed no difference in carbon, oxygen and silicon concentrations between the wing and stripe areas.

The strong donor bound exciton (D^{0}X) PL peak emitted from the wing material had a FWHM $<$ 300 µeV (below the resolution of the equipment); the analogous peak for the stripe material had a FWHM of 12 meV, as shown in Fig. 11. The former peak is a hallmark of the markedly lower strain in the wing material, and it is comparable to that emitted by completely relaxed homoepitaxial GaN film grown on bulk GaN crystals [45]. A downshift in the D^{0}X peak of 5 meV in the stripes with respect to the wing is due to the larger tensile strain in the former. Some shift in this peak could also be due to unintentional doping; however, analysis of the results of SIMS measurements revealed no evidence for this factor. The broadening of the D^{0}X line in the stripe material and its decreased intensity relative to that of the peak from the wing material is due both to the inhomogeneous strain and the higher dislocation density in the former [41].
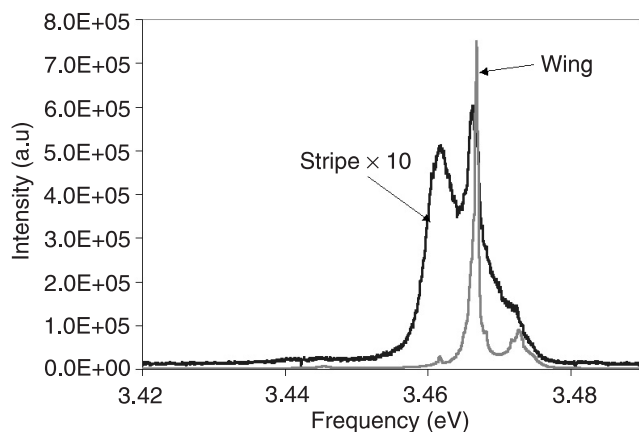

Fig. 11. Photoluminescence (PL) spectra taken from the wing and stripe region of an uncoalesced PE GaN film. Note the FWHM value for the wing peak is < 300 µeV.

4. Conclusions

Maskless pendeo-epitaxy of uncoalesced GaN(0001) produces crystallographically relaxed wing regions, the D^{0}X PL signal of which emits strongly and has a FWHM less that < 300 µeV. These two characteristics are due to the suspended and relaxed nature of these regions. The stresses generated in the stripe regions are due mainly to mismatch in the coefficients of thermal expansion between the GaN film and the SiC substrate. The resulting strains result in crystallographic tilt of the wing material on cooling from the growth temperatures. Growth rates in the [0001] and [11$\bar{2}$0] directions are different because of the different growth mechanisms and the differences in thermal stability

of each surface and can be controlled by growth temperature and the NH$_3$/TEG molar gas ratio. Adatom diffusion is limited on the GaN(0001) surface at the 1100°C temperature normally used for PE growth due to decomposition of this surface. However, the diffusion is sufficient such that the adsorbed species reach the heterogeneous steps generated at the terminations of screw and mixed dislocations with the growth surface and subsequently result in the formation of spiral growth hillocks that propagate laterally across the surfaces of the stripe and wing regions. A reduction in growth temperature reduces the lateral growth rate; however, it also results in smooth, stepped, hillock-free (0001) PE surface with atomically smooth (11$\bar{2}$0) sidewalls.

Acknowledgements

References

1. D. Kapolnek, S. Keller, R. Vetury, R.D. Underwood, P. Kozodoy, S.P. DenBaars, and U.K. Mishra, "Anisotropic epitaxial lateral growth in GaN selective area epitaxy", *Appl. Phys. Lett.* **71**, 1204–1206 (1997).
2. H. Marchand, J.P. Ibbetson, P.T. Fini, S. Chichibu, S.J. Rosner, S. Keller, S.P. DenBaars, J.S. Speck, and U.K. Mishra, "Structural and optical properties of low-dislocation-density GaN laterally overgrown by metalorganic chemical vapour deposition", *25th Int. Symp. Compound. Semiconductors*, Nara, Japan, 1998.
3. I.H. Kim, C. Sone, O.H. Nam, Y.J. Park, and T. Kim, "Crystal tilting in GaN grown by pendeopitaxy method on sapphire substrates", *Appl. Phys. Lett.* **75**, 4109–4111 (1999).
4. A. Sakai, H. Sunakawa, A. Kimura, and A. Usui, "Self-organised propagation of dislocations in GaN films during epitaxial lateral overgrowth", *Appl. Phys. Lett.* **76**, 442–444 (2000).
5. X. Zhang, P.D. Dapkus, and D.H. Rich, "Lateral epitaxy overgrowth of GaN with NH$_3$ flow rate modulation", *Appl. Phys. Lett.* **77**, 1496–1498 (2000).
6. O.H. Nam, M.D. Bremser, T.S. Zheleva, and R.F. Davis, "Lateral epitaxy of low defect density GaN layers via organometallic vapour phase epitaxy", *Appl. Phys. Lett.* **71**, 2638–2640 (1997).
7. O.H. Nam, T.S. Zheleva, M.D. Bremser, and R.F. Davis, "Lateral epitaxial overgrowth of GaN films on SiO$_2$ areas via metalorganic vapour phase epitaxy", *J. Elect. Mater.* **27**, 233–237 (1998).
8. R.F. Davis, T. Gehrke, K.J. Linthicum, T.S. Zheleva, E.A. Preble, P. Rajagopal, C.A. Zorman, and M. Mehregany, "Pendeo-epitaxial growth of thin films of gallium nitride and related materials and their characterisation", *J. Cryst. Growth* **225**, 134–140 (2001).

9. R.S.Q. Fareed, J.W. Yang, J. Zhang, V. Adivarahan, V. Chaturvedi, and M.A. Khan, "Vertically faceted lateral overgrowth of GaN on SiC with conducting buffer layers using pulsed metalorganic chemical vapour deposition", *Appl. Phys. Lett.* **77**, 2343–2345 (2000).

10. T. Gehrke, K.J. Linthicum, E. Preble, P. Rajagopal, C. Ronning, C. Zorman, M. Mehregany, and R. F. Davis, "Pendeo-epitaxial growth of gallium nitride on silicon substrates", *J. Electron. Mater.* **29**, 306–310 (2000).

11. K. Linthicum, T. Gehrke, D. Thomson, E. Carlson, P. Rajagopal, T. Smith, D. Batchelor, and R.F. Davis, "Pendeo-epitaxy of gallium nitride thin films", *Appl. Phys. Lett.* **75**, 196–198 (1999).

12. D.B. Thomson, T. Gehrke, K.J. Linthicum, P. Rajagopal, and R.F. Davis, "Ranges of deposition temperatures applicable for metalorganic vapour phase epitaxy of GaN films via the technique of pendeo-epitaxy", *MRS Internet J. Nitride Semicond. Res.* **4S1**, G3.7 (1999).

13. T. Zheleva, S. Smith, D. Thomson, and K. Linthicum, "Pendeo-epitaxy- a new approach for lateral growth of gallium nitride films", *J. Electron. Mater.* **28**, L5–L8 (1999).

14. T. Gehrke, K.J. Linthicum, E.A. Preble, and R.F. Davis, "Pendeo-epitaxy of gallium nitride and aluminium nitride films and heterostructures on silicon carbide substrates", *MRS Internet J. Nitride Semicond. Res.* **5S1**, W2.4 (2000).

15. T. Gehrke, K.J. Linthicum, D.B. Thomson, P. Rajagopal, A.D. Batchelor, and R.F. Davis, "Pendeo-epitaxy of gallium nitride and aluminium nitride films and heterostructures on silicon carbide substrates", *MRS Internet J. Nitride Semicond. Res.* **4S1**, G3.2 (1999).

16. P. Fini, H. Marchand, J.P. Ibbetson, S.P. DenBaars, U.K. Mishra, and J.S. Speck, "Determination of tilt in the lateral epitaxial overgrowth of GaN using X-ray diffraction", *J. Cryst. Growth* **209**, 581–590 (2000).

17. S. Tomiya, K. Finato, T. Asatsuma, T. Hino, S. Kijima, T. Asano, and M. Ikeda, "Dependence of crystallographic tilt and defect distribution on mask material in epitaxial lateral overgrown GaN layers", *Appl. Phys. Lett.* **77**, 636–638 (2000).

18. P. Fini, A. Munkholm, C. Thompson, G.B. Stephenson, J.A. Eastman, M.V. Ramana Murty, O. Auciello, L. Zhao, S.P. DenBaars, and J.S. Speck, "In-situ, real-time measurement of wing tilt during lateral epitaxial overgrowth of GaN", *Appl. Phys. Lett.* **76**, 3893–3895 (2000).

19. H. Marchand, J.P. Ibbetson, P.T. Fini, S. Keller, S.P. DenBaars, J.S. Speck, and U.K. Mishra, "Mechanisms of lateral epitaxial overgrowth of gallium nitride by metalorganic chemical vapour deposition", *J. Cryst. Growth* **195**, 328–332 (1998).

20. W.C. Johnson, J.B. Parsons, and M.C. Crew, *J. Phys. Chem.* **36**, 2651 (1932).

21. A. Rebey, T. Boufaden, and B. El Jani, "In situ optical monitoring of the decomposition of GaN thin films", *J. Cryst. Growth* **203**, 12 (1999).

22. D.D. Koleske, A.E. Wickenden, R.L. Henry, M.E. Twigg, J.C. Culbertson, and R.J. Gorman, "Enhanced GaN decomposition at MOVPE pressures", *MRS Internet J. Nitride Semicond. Res.* **S1**, G3.70 (1999).

23. D.D. Koleske, A.E. Wickenden, R.L. Henry, M.E. Twigg, J.C. Culbertson, and R.J. Gorman, "Enhanced GaN decomposition in H_2 near atmospheric pressures", *Appl. Phys. Lett.* **73**, 2018–2020 (1998).

24. D.D. Koleske, A.E. Wickenden, and R.L. Henry, "GaN decomposition in ammonia", *MRS Internet J. Nitride Semicond.* **5S1**, W3.64 (1999).

25. M. Mayumi, F. Satoh, Y. Kumagai, K. Takemoto, and A. Koukitu, "In-situ gravimetric monitoring of decomposition rate from GaN epitaxial surface", *Jpn. J. Appl. Phys.* **39**, L707–L709 (2000).

26. D.D. Koleske, A.E. Wickenden, R.L. Henry, W.J. DeSisto, and R.J. Gorman, "Growth model for GaN with comparison to structural, optical and electrical properties", *J. Appl. Phys.* **84**, 1998 (1998).

27. O. Briot, S. Clur, and R.L. Aulombard, "Competitive adsorption effects in the metalorganic vapour phase epitaxy of GaN", *Appl. Phys. Lett.* **71**, 1990–1992 (1997).

28. O. Briot, J.P. Alexis, M. Tchounkeu, and R.L. Aulombard, "Optimisation of the MOVPE growth of GaN on sapphire", *Mater. Sci. Eng.* **B43**, 147–153 (1997).

29. C.J. Sun, P. Kung, A. Saxler, H. Ohsato, E. Bigan, M. Razeghi, and D.K. Gaskill, "Thermal stability of GaN thin films grown on (0001) Al_2O_3, (11$\bar{2}$0) Al_2O_3 and (0001)$_{Si}$ 6H-SiC substrates", *J. Appl. Phys.* **76**, 236–241 (1994).

30. K. Hiramatsu, S. Itoh, H. Amano, I. Akasaki, N. Kuwano, T. Shiraishi, and K. Oki, "Growth mechanisms of GaN grown on sapphire with AlN buffer layers by MOVPE", *J. Cryst. Growth* **115**, 628–633 (1991).

31. J.E. Northrup and J. Neugebauer, "Theory of GaN(10$\bar{1}$0) and (11$\bar{2}$0) surfaces", *Phys. Rev.* **B53**, R10477–10480 (1996).

32. D. Kapolnek, X.H. Wu, B. Heying, S. Keller, B.P. Keller, U.K. Mishra, S.P. DenBaars, and J.S. Speck, "Structural evolution in epitaxial metalorganic chemical vapour deposition grown GaN films on sapphire", *Appl. Phys. Lett.* **67**, 1541–1543 (1995).

33. H. Heinke, V. Kirchner, S. Einfeldt, and D. Hommel, "Analysis of the defect structure of epitaxial GaN", *Phys. Stat. Sol. (a)* **176**, 391–395 (1999).

34. A.M. Roskowski, P.Q. Miraglia, E.A. Preble, S. Einfeldt, and R.F. Davis, "Surface instability and associated roughness during conventional and pendeo-epitaxial growth of GaN films via MOVPE", accepted for publication.

35. W.K. Burton, N. Cabrera, and F.C. Frank, "The growth of crystals and the equilibrium structure of their surfaces", *Philos. Trans. R. Soc. London, Ser.* **A243**, 299 (1951).

36. V. Merlin, T.M. Duc, G. Younes, Y. Monteil, V. Souliere, and P. Regreny, "Misorientation effect on monolayer terrace topography of (100) InP substrates annealed under a Ph_3/H_2 ambient and homoepitaxial layers grown by metalorganic chemical vapour deposition", *J. Appl. Phys.* **78**, 5048–5052 (1995).

37. A. Zauner, J.L. Weyher, M. Plomp, V. Kirilyuk, I. Grzegory, W.J.P. v. Enckevort, J.J. Schermer, P.R. Hageman, and P.K. Larsen, "Homo-epitaxial GaN growth on exact and misorientated single crystals: suppression of hillock formation", *J. Cryst. Growth* **210**, 435–443 (2000).

38. S. Einfeldt, A.M. Roskowski, E.A. Preble, and R.F. Davis, "Strain and crystallographic tilt in uncoalesced GaN layers grown by maskless pendeo-epitaxy", *Appl. Phys. Lett.* **80**, 563–566 (2002)

39. H. Heinke, private communication.

40. C. Kisielowski, J. Kruger, S. Runimov, T. Suski, J.W. Ager III, E. Jones, Z. Liliental-Weber, M. Ruben, E.R. Weber, M.D. Bremser, and R.F. Davis, "Strain-related phenomena in GaN thin films", *Phys. Rev.* **B54**, 17745–17753 (1996).

41. U.T. Schwarz, P.J. Schuck, R.D. Grober, A.M. Roskowski, S. Einfeldt, and R.F. Davis, "Micro-Raman and micro-photoluminescence studies of strain relaxation in pendeo GaN on SiC". (to be published)

42. P. Perlin, J. Camassel, W. Knap, T. Taliercio, J.C. Chervin, T. Suski, I. Grzegory, and S. Porowski, "Investigation of longitudinal-optical phonon-plasmon coupled modes in highly conducting bulk GaN", *Appl. Phys. Lett.* **67**, 2524–2526 (1995).

43. F. Bertram, T. Riemann, J. Christen, A. Kaschner, A. Hoffmann, C. Thomsen, K. Hiramatsu, T. Shibata, and N. Sawaki, "Strain relaxation and strong impuritiy incorpora-tion in epitaxial laterally overgrown GaN: direct imaging of different growth domains by cathodluminescence microscopy and micro-Raman spectroscopy", *Appl. Phys. Lett.* **74**, 359–361 (1999).

44. J.W.P. Hsu, M.J. Matthews, D. Abusch-Magder, R.N. Kleiman, D.V. Lang, S. Richter, S.L. Gu, and T.F. Kuech, "Spatial variation of electrical properties in lateral epitaxially overgrown GaN", *Appl. Phys. Lett.* **79**, 761–763 (2001).

45. C. Kirchner, V. Schwegler, F. Eberhard, M. Kamp, K.J. Ebeling, K. Kornitzer, T. Ebner, K. Thonke, R. Sauer, P. Prystawko, M. Leszczynski, I. Grzegory, and S. Porowski, "Homoepitaxial growth of GaN by metalorganic vapour phase epitaxy: A benchmark for GaN technology", *Appl. Phys. Lett.* **75**, 1098–1100 (1999).